ELSEVIER

Journal of Alloys and Compounds 330–332 (2002) 617–621

Journal of ALLOYS AND COMPOUNDS

www.elsevier.com/locate/jallcom

Effects of fluorination on the hydriding and electrochemical properties of a gas-atomized Zr-based hydrogen storage alloy

S.S. Huang, H.J. Chuang, S.L.I. Chan*

Institute of Materials Science and Engineering, National Taiwan University, Taipei, Taiwan

Abstract

The feasibility of using fluorination to improve the charging/discharging abilities of a Zr-based AB_2 hydrogen storage alloy prepared by atomization has been evaluated. Electrodes produced by the as-received powder have only 73% of the discharge capacity of that prepared from cast alloy. Because of the difference in cooling rate, larger as-atomized powder consisted of a profoundly dendritic structure on the surface, while the smaller ones tended to have a smoother surface. After F treatment for 20 or 60 min, the powder possessed better activation properties and discharge capacities, although the hydrogenation ability did not improve much. F treatment also enhanced the rate capability of alloy electrodes. It was found that the F ions preferably dissolved the oxide layer on the powder surface, and formed channels connecting the surface Ni-rich layers formed during the treatment. All these factors contributed to the improvement of the electrochemical properties of the atomized powder.

Keywords: Gas-atomized hydrogen storage alloy; Fluorination treatment; Hydrogenation; Electrochemical properties

1. Introduction

The performance of the negative electrode in a nickel–metal hydride (Ni/MH_x) battery is highly related to the chemical composition of the hydrogen storage alloy used in the electrode. In this respect, the degree of chemical homogeneity of the alloy is of special concern. The application of inert gas atomization for alloy fabrication in recent years helps in minimizing the effect of segregation. Other advantages of inert gas atomization, as compared to that of ingot casting, include large-scale production, easy control of the particles sizes and a lower self-discharge rate. However, the powder produced by the rapid solidification in the atomization process is reported to have a lower rate capability, a reduction in the hydrogen storage ability and a slower activation rate of discharge [1,2]. These authors attributed the poor performance to the presence of a passive layer consisting of oxides and/or an amorphous structure. It has also been shown that the gas-atomized powder could recover its ability to absorb hydrogen after annealing, so the composition changes inside the gas-atomized powder may play a role in the hydrogen storage ability of the alloy [3].

To improve the activation of negative electrode materials, treatment using a F-containing aqueous solution was suggested which can raise the activity of the metal hydride, and prolong the storage life of the alloy in air. There are many reports showing that HF treatment is beneficial to the performance of hydrogen storage alloys [4–7]. For example, when a Ti–Zr-based hydrogen storage alloy with a small content of La was treated with HF [6], it still maintained good electrochemical properties after 6 months storage in air and water. This beneficial effect was due to a protective LaF_3 layer on the surface of the alloy induced by HF treatment [6]. In another study, the alloy $Zr(V_{0.4}Ni_{0.6})_{2.4}$ was treated with HF solution, and the electrochemical properties and hydrogenation ability increased substantially [7]. The surface structure of an HF-treated AB_2 alloy was observed by TEM (transmission electron microscopy) and AES (Auger spectroscopy) [8]. The specimen was deliberately oxidized and then treated with dilute HF. TEM revealed the dissolution of oxide scale, but some nanocrystalline and amorphous structure consisting mainly of nickel and manganese also appeared. These findings were supported by their AES study where an 8 nm Ni-rich layer was detected on the powder surface.

While HF treatment has been applied successfully to conventional arc-melted hydrogen storage alloys, its effects on gas-atomized powder are unclear. One of the reasons is that the structure of a gas-atomized hydrogen

*Corresponding author.

0925-8388/02/$ – see front matter
PII: S0925-8388(01)01457-8

storage alloy is more complex than that of a conventional arc-melted alloy. In this study, hydrogen absorption tests and charge/discharge tests were used to identify the reasons for passivation in a gas-atomized alloy powder. HF treatment was applied to a gas-atomized powder, and its effects on the electrochemical properties and storage ability were evaluated.

2. Experimental

A Ti–Zr–Ni-based AB_2 hydrogen storage alloy was used in the study. The alloy powder was prepared by vacuum inductive melting, followed by atomization under high-purity argon. The conditions for gas atomization were: taping temperature 1500°C, atomization time 13.5 g/s, nozzle diameter 3 mm and nozzle pressure 30 bar. For comparison, an ingot with the same composition was prepared by VIM. The ingot was remelted several times to ensure homogeneity, and then pulverized by hydride–dehydride (HDH) processes. Compositions of the atomized powder and cast/HDH powder were analyzed by an inductively coupled plasma spectrometer (ICP). Since the response to HF treatment varies with particle size [9], the powders were passed through #400, #270 and #140 seives, and only the largest powders were used in the hydrogenation and electrochemical characterization study.

The fluorination treatment included a 5-min rinse in HCl, following by immersion in HF for 20 or 60 min at room temperature. The solution consisted of 0.014 N HF, and 400 ml of this solution was used for every 10 g of alloy powder. The solution was stirred continuously during treatment, so that the powder could react with the solution uniformly. A pH meter was used to continuously monitor the variation of the acidity of the HF solution. The changes in the oxygen content and surface area of the treated alloy powder were measured. Scanning electron microscopy (SEM) and Auger spectroscopy depth profiling were employed to study the surface layers of the powders before and after F treatment. Pressure–composition–isotherms (*P–C–I* curves) for the alloy powders were measured with a Sieverts-type apparatus.

To produce the electrodes for electrochemical property evaluations, the alloy powders were mixed with a double weight of nickel powder, ethyl alcohol and binder (60% PTFE dispersion). The mixture was then plated onto a nickel mesh and cold pressed under 155–175 MPa before baking in vacuum. Each test cell consisted of one alloy electrode enclosed by a non-woven nylon cloth separator and two $Ni(OH)_2$/NiOOH counter electrodes. In these charge/discharge tests, the electrodes were tested in a closed cell and measured at the same current density (15 mA/g). The cut-off voltage was 1.0 V to the $Ni(OH)_2$/NiOOH electrode.

Table 1
Chemical compositions of alloy powders (wt%)

Sample	Ti	Zr	Ni	V	Cr	Mn	Fe	Al
A	13.1	23.8	Bal.	10.5	5.9	6.0	5.9	2.7
B	13.1	23.7	Bal.	10.4	6.0	6.1	5.8	2.7

A, arc-melted; B, atomized.

3. Result and discussion

The chemical compositions of the atomized powder and cast/HDH powder as analyzed by ICP are shown in Table 1. It can be seen that the two powders were identical in terms of composition. Figs. 1 and 2 show SEM micrographs of the as-received atomized powder and the cast/HDH powder, respectively. The atomized powders were spherical, with a range of sizes. The average particle size was measured by a laser light scattering particle size analyzer and was found to be 35 μm. It can also be seen

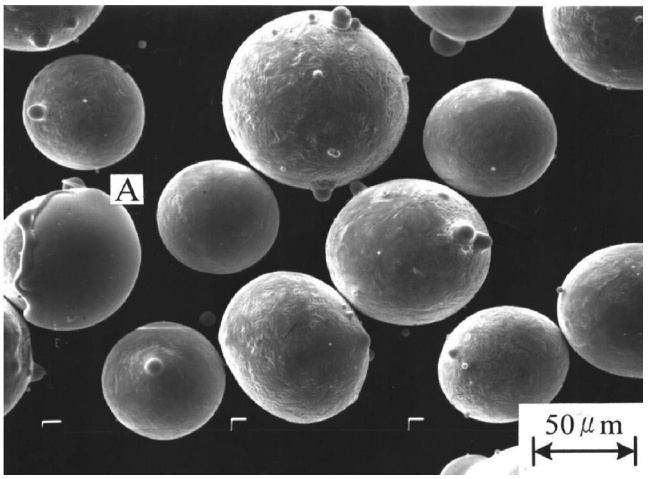

Fig. 1. Micrograph of as-received atomized powders.

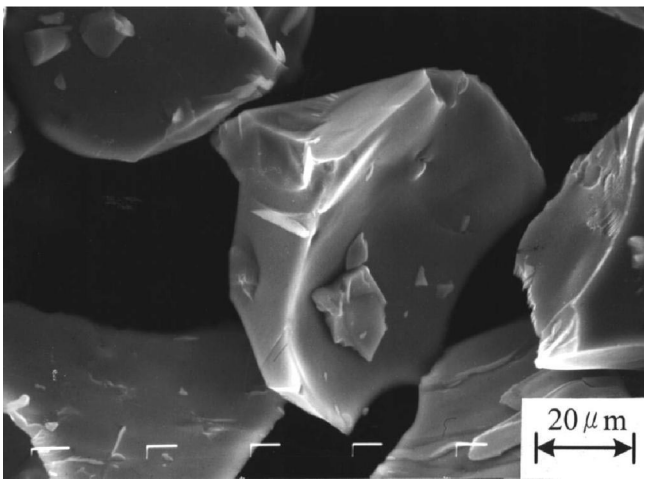

Fig. 2. Micrograph of the arc-melted alloy powders.

from Fig. 1 that dendrite structures were formed on the surfaces of larger powders, while the surfaces of the smaller powders tended to be smoother and featureless. This phenomenon can be explained by the differences in cooling rate of large and small powders during solidification. For large powders, the cooling rate was relatively slow and there was time for the dendrites to form during solidification. The higher cooling rate of the small powders inhibited the growth of the dendrites, and it is likely that this surface was largely amorphous [2]. As discussed in the previous section, only large powders were used in the hydrogenation and electrochemical characterization studies. The particle size of these powders was measured and their average diameter was found to be 72 μm. The gas-atomized powder A as indicated in Fig. 1 touched a liquid droplet after solidification. Because of the fast solidification rate, the droplet solidified onto the powder and formed a cap-like layer on the powder. The surface of the cap appeared to be similar to the surface layer of smaller gas-atomized powder. For the cast/HDH powder (Fig. 2), the shape was irregular with many facets, each showing a cleavage type of surface.

Fig. 3 shows a SEM micrograph of large atomized powder after 60-min treatment in HF solution. The sites of attack by HF were closely related to the dendritic structure on the surface, where ditches along the boundaries of the dendrite structure were found. At site A of Fig. 3, however, the smooth layer on the top of the powder cannot be attacked by fluoride ions even after a 60-min HF solution treatment. This was similar to the result of HF treatment of the smaller gas-atomized powder [9], where the amorphous layer on the surface of the small powder was immune to fluoride attack. By comparing the AES depth profiles of as-received and HF-treated powders, it was found that the surface oxide was largely reduced, with an increase in Ni concentration close to the surface.

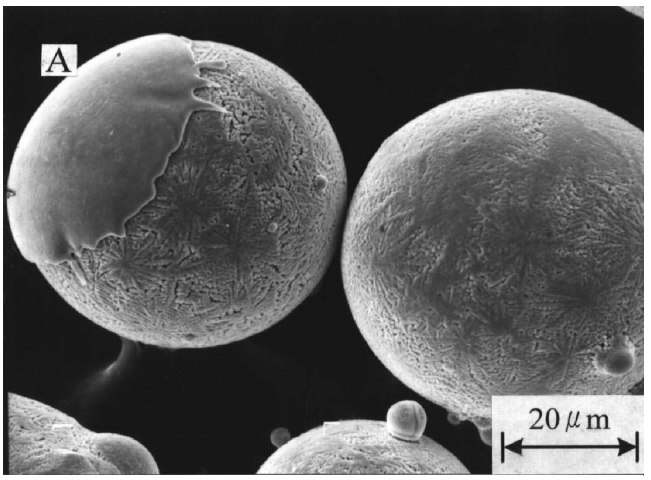

Fig. 3. Surface appearance of the F-treated atomized powder showing a 'cap' (A) on the powder.

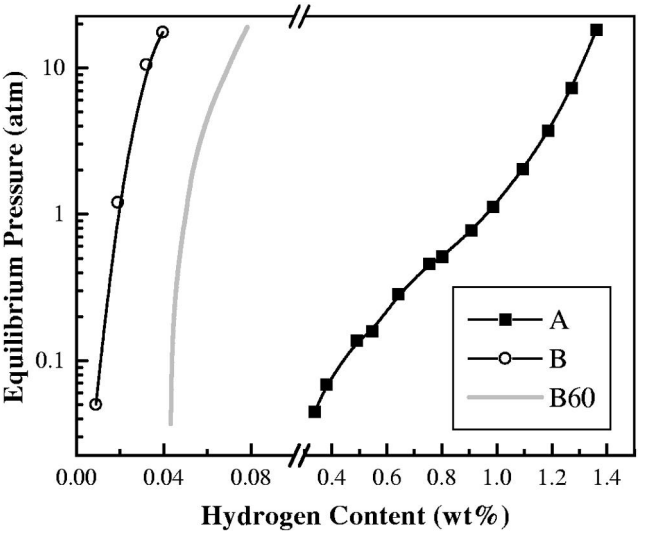

Fig. 4. *P–C–I* curves of hydrogen storage alloy. (A) Arc-melted alloy (M.D. 91.0 μm). (B) Atomized powder (M.D. 36.2 μm). (B60) Atomized powder after 60-min F treatment.

The hydrogen storage ability of the gas-atomized powder is shown in Fig. 4. The arc-melted alloy (sample A) absorbed the maximum amount of hydrogen (about 1.4 wt%), and all other samples absorbed less than 0.1 wt% hydrogen. This confirmed our previous work [2] where the alloy produced by the atomization process lost its ability to absorb hydrogen. HF treatment can dissolve some dendritic boundaries to increase the amount of fresh area on the powder surface, but the effect on the hydrogen capacity was small. It is possible that there was still a thin amorphous structure on the surface that was immune to HF attack, hence hindering the entry of the hydrogen into the powder.

The activation curves of cast/HDH alloy and the as-received atomized powder are shown in Fig. 5. The discharge capacity of the arc-melted alloy (sample A) reached 285 mAh/g. Better activity was also obtained as compared to that of gas-atomized powder. The as-received powder has a surface covered with oxides and/or an amorphous structure, and it possessed only three-quarters of the discharge capacity of the arc-melted alloy. However, HF treatment improved the discharge ability significantly (Fig. 6). After HF treatment, the test cell reached the full activation state within four charging/discharging cycles, and the maximum discharge capacity of the atomized powder after 20-min treatment increased from 213 to 263 mAh/g. The atomized powder treated for 60 min showed the best result, where the capacity (305 mAh/g) was more than that of a cast/HDH alloy. Thus, 60-min HF treatment is a very effective way to restore the electrochemical properties of atomized powders. It is suggested that the treatment removed some surface oxide and created channels linking the inside of the alloy powder to the outside

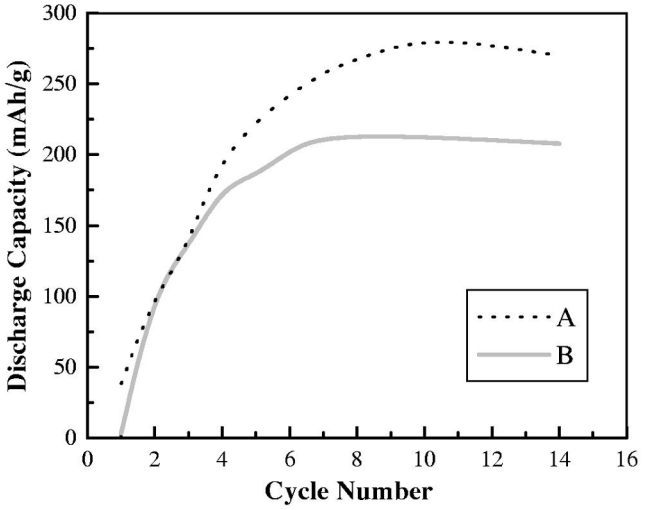

Fig. 5. Activation curves of (A) the arc-melted alloy and (B) as-received atomized powder.

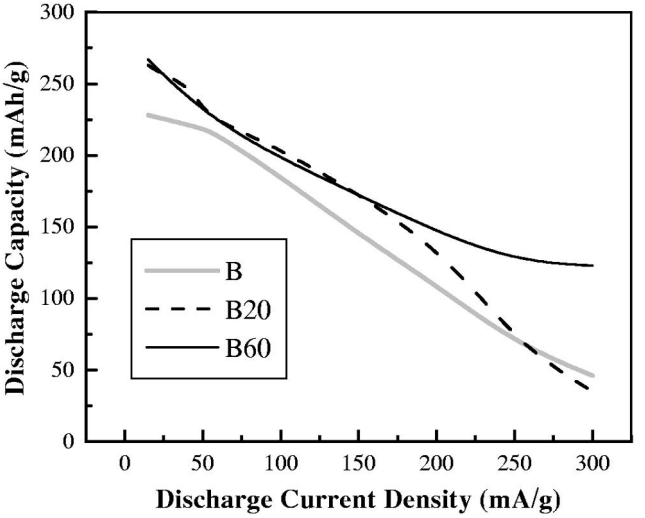

Fig. 7. Discharge capacity as a function of discharge current. (B) Atomized powder. (B20) After 20-min F treatment. (B60) After 60-min F treatment.

layer. These channels can transport the hydrogen effectively. The enriched Ni layer may also contribute to the improvement by acting as a catalyst for electrochemical reactions. The rate capacities of the treated alloy powders were also studied. It was found that the rate capacity was largely improved by HF treatment (Fig. 7). Again, 60-min treatment was found to be more effective.

The difference between gas–solid hydrogenation and electrochemical hydrogenation for the HF-treated atomized powder was quite considerable. A similar observation was reported in our previous paper and it was suggested that the difference was due to the kinetics of the reactions in these two situations [2].

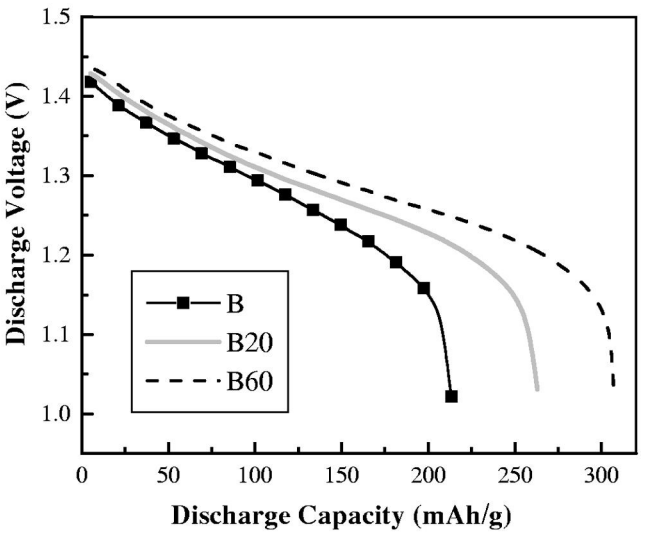

Fig. 6. Discharge voltage characteristics of alloy electrodes. (B) Atomized powder. (B20) After 20-min F treatment. (B60) After 60-min F treatment.

4. Conclusions

Inert gas atomization was used to produce hydrogen storage alloy powder. It was found that the surface morphology of the powders produced depends on the size of the powder. Because of the difference in cooling rate, larger as-atomized powder consisted of a profoundly dendritic structure on the surface, while the smaller powders tended to have a smoother surface. HF treatment was applied to the gas-atomized powder. Electrodes produced by the as-received atomized powder have only 73% of the discharge capacity of those prepared from cast alloy, but after HF treatment the capacity improved substantially. It was found that F ions preferably dissolved the oxide on the powder surface, and a Ni-rich layer was formed on the surface. Flourination also created ditches along the dendrites, which provided channels connecting the core of the powder to the surface Ni-rich layers. The gas–solid hydrogenation ability, however, did not improve much after fluorination.

References

[1] H.S. Lim, G.R. Zelter, D.U. Allison, R.E. Haun, J. Power Sources 66 (1997) 101.
[2] H.J. Chuang, S.S. Huang, C.Y. Ma, S.L.I. Chan, J. Alloys Comp. 285 (1999) 284.

[3] R.C. Bowman Jr., C. Witham, B. Fultz, B.V. Ratnakumar, T.W. Ellis, I.E. Anderson, J. Alloys Comp. 253/254 (1997) 613.
[4] F.-J. Liu, G. Sandrock, S. Suda, J. Alloys Comp. 190 (1992) 57.
[5] F.-J. Liu, G. Sandrock, S. Suda, Mater. Res. Soc. Jpn. 18B (1994) 1237.
[6] F.-J. Liu, S. Suda, J. Alloys Comp. 231 (1995) 666.
[7] X.-P. Gao, P.W. Shen, J. Alloys Comp. 235 (1996) 225.
[8] M. Backhaus-Ricoult, B. Knosp, J. Alloys Comp. 253/254 (1997) 492.
[9] S.S. Huang, S.L.I. Chan, to be published.